0026-895X/99/020404-10$3.00/0

MOLECULAR PHARMACOLOGY, **56:**404–413 (1999).

Point Mutations at N434 in D1-S6 of μ1 Na^+ Channels Modulate Binding Affinity and Stereoselectivity of Local Anesthetic Enantiomers

CARLA NAU, SHO-YA WANG, GARY R. STRICHARTZ, and GING KUO WANG

Department of Anesthesia Research Laboratories, Brigham and Women's Hospital, Harvard Medical School, Boston, Massachusetts (C.N., G.R.S, G.K.W.), and Department of Biological Sciences, State University of New York at Albany, Albany, New York (S.-Y.W.)

Received December 31, 1998; accepted April 30, 1999

This paper is available online at http://www.molpharm.org

ABSTRACT

Voltage-gated Na^+ channels are the primary targets of local anesthetics (LAs). Amino acid residues in domain 4, transmembrane segment 6 (D4-S6) form part of the LA binding site. LAs inhibit binding of the neurotoxin batrachotoxin (BTX). Parts of the BTX binding site are located in D1-S6 and D4-S6. The affinity of BTX-resistant Na^+ channels mutated in D1-S6 (μ1-N434K, μ1-N437K) toward several LAs is significantly decreased. We have studied how residue μ1-N434 influences LA binding. By using site-directed mutagenesis, we created mutations at μ1-N434 that vary the hydrophobicity, aromaticity, polarity, and charge and investigated their influence on state-dependent binding and stereoselectivity of bupivacaine. Wild-type and mutant channels were transiently expressed in human embryonic kidney 293t cells and investigated under whole-cell voltage-clamp. For resting channels, bupivacaine enantiomers showed a higher potency in all mutant channels compared with wild-type channels. These changes were not well correlated with the physical properties of the substituted residues. Stereoselectivity was small and almost unchanged. In inactivated channels, the potency of bupivacaine was increased in mutations containing a quadrupole of an aromatic group (μ1-N434F, μ1-N434W, μ1-N434Y), a polar group (μ1-N434C), or a negative charge (μ1-N434D) and was decreased in a mutation containing a positive charge (μ1-N434K). In mutation μ1-N434R, containing the positively charged arginine, the potency of S(−)-bupivacaine was selectively decreased, resulting in a stereoselectivity (stereopotency ratio) of 3. Similar results were observed with cocaine but not with RAC 109 enantiomers. We propose that in inactivated channels, residue μ1-N434 interacts directly with the positively charged moiety of LAs and that D1-S6 and D4-S6 form a domain-interface site for binding of BTX and LAs in close proximity.

Na^+ channels are transmembrane proteins that govern voltage-dependent modulation of Na^+ ion permeability of excitable membranes. Mammalian Na^+ channels consist of one large α subunit and one or two smaller β subunits. The α subunit is formed by four homologous domains (D1-D4), each containing six transmembrane segments (S1-S6; Catterall, 1995).

Local anesthetics (LAs) block the propagation of action potentials in excitable membranes by binding to voltage-gated Na^+ channels. LA binding, as defined by the potency for inhibiting ionic Na^+ current, is modulated by channel state. Resting channels have a low affinity for LAs; open and inactivated channels have a higher affinity. The changes between low- and high-affinity channels can be explained by voltage-dependent conformational changes of the LA binding site (modulated receptor hypothesis: Hille, 1977; Hondeghem and Katzung, 1977).

Amino acid residues in D4-S6 have been identified as molecular determinants of LA binding (Ragsdale et al., 1994). Mutations F1764A and Y1771A of rat brain IIA Na^+ channels had the strongest effect in decreasing the affinity of open and inactivated channels toward the LA etidocaine. Because these residues are oriented on the same face of the α helix, it was suggested that they face the channel pore and that they interact with LA molecules through hydrophobic or cation-π electron interactions. The selectivity filter of Na^+ channels was shown to participate in antiarrhythmic drug binding and access to the site as well and therefore was located adjacent to D4-S6 (Sunami et al., 1997).

The neurotoxin batrachotoxin (BTX) also binds to voltage-gated Na^+ channels. Upon binding, BTX shifts the activation process toward hyperpolarizing potentials and inhibits fast and slow inactivation. LAs are allosteric inhibitors of BTX binding. Interactions with the closed state of BTX-modified Na^+ channels are hampered for LAs, but they bind readily to the open state (Wang and Wang, 1992) without displacing BTX from its receptor (Zamponi et al., 1993).

This study was supported by National Institutes of Health Grants GM35401 and GM48090 (to G.K.W and S.-Y.W.) and by a stipend of the Deutsche Forschungsgemeinschaft (to C.N).

ABBREVIATIONS: LA, local anesthetic; BTX, batrachotoxin; HEK, human embryonic kidney.

Photoaffinity labeling (Trainer et al., 1996) and subsequent site-directed mutagenesis studies (Wang and Wang, 1998) have revealed three residues in D1-S6 that are probably involved in BTX binding: the conserved μ1-N434 residue and the two adjacent residues μ1-I433 and μ1-L437 (Wang and Wang, 1998). Mutations μ1-I433K, μ1-N434K, μ1-N434R, and μ1-L437K rendered the Na^+ channels completely insensitive to BTX. A recent study investigating the interactions of BTX with molecular determinants of the LA binding site showed that parts of the BTX binding site are located in D4-S6 as well (Linford et al., 1998), sharing overlapping but nonidentical molecular determinants with the LA binding site in D4-S6. A domain-interface allosteric model of BTX binding, similar to the domain-interface model of Ca^{2+}-channel drug binding (interface of D3-S6 and D4-S6; Hockerman et al., 1997), was proposed for BTX binding to the Na^+ channel, with its dimethylpyrrolidone carboxylic acid group directed toward D1-S6 and its steroid moiety toward D4-S6.

A study investigating LA action on BTX-resistant μ1 Na^+ channels showed that LA binding was reduced in mutations μ1-N434K and μ1-L437K (Wang et al., 1998), most strongly for the charged LA QX314 and minimally for the neutral LA benzocaine. In mutation μ1-N434D, the binding affinity was increased for several LAs at a holding potential of −100 mV. The investigators concluded that residues at the putative BTX binding site in D1-S6 are critical for LA binding as well and that D1-S6 and D4-S6 align adjacently along the Na^+ permeation pathway.

With the present study, we sought to investigate more rigorously how residues at the putative BTX binding site in D1-S6 interact with local anesthetics. We used site-directed mutagenesis to make a series of amino acid substitutions in position μ1-N434 that vary the hydrophobicity, aromaticity, polarity, and charge at this site. As local anesthetic probes, we chose the enantiomers of bupivacaine, cocaine, and RAC 109, because stereoisomers have been useful tools in receptor recognition and receptor mapping. However, unmodified Na^+ channels display only weak stereoselectivity toward bupivacaine enantiomers (Wang and Wang, 1992). On the other hand, the affinity of BTX-modified channels for S(−)-bupivacaine is 30 times higher than that for R(+)-bupivacaine (Wang and Wang, 1992), which suggests that, in BTX-activated channels, the chiral part of bupivacaine might be oriented toward the BTX binding site or toward sites that are allosterically changed in the presence of BTX. The results of this study support the idea that in inactivated channels, residue μ1-N434 in D1-S6 interacts directly with the positively charged moiety of LAs.

Materials and Methods

Site-Directed Mutagenesis and Transient Expression. The methods of site-directed mutagenesis have been described (Wang and Wang, 1997). Mutagenesis of μ1 was performed with μ1-pcDNA1/amp by means of the Transformer Site-Directed Mutagenesis Kit (Clontech, Inc., Palo Alto, CA). Two primers (a mutagenesis primer and a restriction primer) were synthesized and used to generate the desired mutants. The restriction primer was 5′-CTGGCGGCCG*GTCGAC*CATGCATCTAG-3′, in which the wild-type *Xho*I site has been changed to a *Sal*I site (italic). In vitro synthesis was performed for a total of 4 h, with one addition of deoxynucleoside triphosphates and T4-DNA polymerase during the reaction. The potential mutants were identified by restriction enzyme digestion and confirmed by DNA sequencing with appropriate primers near the mutated region.

The culture of human embryonic kidney (HEK) 293t cells and their transfection by the calcium phosphate precipitation method have been described previously (Cannon and Strittmatter, 1993). Cells were grown to 50% confluence in a Ti25 flask (Falcon 25 cm^2/50 ml; Becton Dickinson Labware, Franklin Lakes, NJ) for transfection. After transfection of μ1-pcDNA1 (10 μg) and reporter plasmid CD8-pih3 m (1 μg) for 15 h, cells were replated in 35-mm culture dishes. Transfected cells were used for experiments within 4 days. Transfection-positive cells were identified by immunobeads (CD-8 Dynabeads; Dynal, Lake Success, NY).

Chemicals and Solutions. Bupivacaine and RAC 109 enantiomers were gifts from Chiroscience Ltd. (Cambridge, UK), Dr. Rune Sandberg (ASTRA Pain Control, Södertälje, Sweden), and the late Dr. Bertil Takman (Astra Pharmaceutical Products, Inc., Worcester, MA). Cocaine enantiomers were obtained from Dr. Rao Rapaka (National Institute on Drug Abuse, Bethesda, MD).

The drugs were dissolved in aqueous solution to give 100-mM stock solutions and were stored at −20°C. Experiments were performed with an external solution containing 150 mM Choline Cl, 2 mM $CaCl_2$, and 10 mM HEPES (adjusted to pH 7.4 with tetramethylammonium hydroxide), and a pipette solution containing 100 mM NaF, 30 mM NaCl, 10 mM EGTA, and 10 mM HEPES (adjusted to pH 7.2 with CsOH). The reversed Na^+ gradient was used to minimize the series resistance artifact, which is less serious with outward currents than with inward currents (Cota and Armstrong, 1989). After a gigaohm seal and a whole-cell voltage-clamp were established, the cells were dialyzed for a minimum of 20 min before data were acquired. Control solutions as well as test solutions were applied with a multiple-barrel perfusion system.

Electrophysiological Technique and Data Acquisition. Na^+ currents transiently expressed in HEK 293t cells were recorded at room temperature (23 ± 2°C) with the whole-cell configuration of the patch-clamp method (Hamill et al., 1981). Patch pipettes were pulled from borosilicate glass tubes (TW150F-3; World Precision Instruments, Sarasota, FL) and heat-polished at the tip to give a resistance of 0.6–1.0 MΩ. Currents were recorded with an Axopatch 200A patch clamp amplifier (Axon Instruments, Foster City, CA), filtered at 5 kHz, sampled at 20 kHz, and stored on the hard disk of an IBM-compatible computer. All experiments were conducted under capacitance cancellation and series-resistance compensation. Series-resistance errors were about 5 mV on average after compensation. Leakage currents were subtracted by the P/-4 method. Liquid junction potentials were <3 mV and were not corrected. pCLAMP 6.0 software (Axon Instruments) was used for acquisition and analysis of currents. Microcal Origin software (Microcal Software, Northampton, MA) was used to perform least-squares fitting and to create figures. Data are presented as mean ± S.E. or fitted value ± S.E. of the fit. An unpaired Student's t test (SigmaStat; Jandel Scientific Software, San Rafael, CA) was used to evaluate the significance of changes in mean values. p Values $< .05$ were considered statistically significant.

Pulse Protocols. It was recently demonstrated that two affinities for LA drugs can be distinguished that correspond to binding to the resting state of Na^+ channels, measured at strongly negative potentials (≤−140 mV), and to the inactivated state of Na^+ channels, measured at less negative potentials (≥−70 mV; Wright et al., 1997). These binding affinities of resting and inactivated channels could be estimated directly for LAs that unbind slowly from inactivated channels with the following voltage pattern (Fig. 1B, inset): a 10-s conditioning prepulse to various potentials was applied to allow binding to reach the steady state; then, a 100-ms interval at the holding potential of −140 mV was inserted before delivery of the test pulse to +30 mV to allow drug-free channels to recover from fast inactivation (Wright et al., 1997). For the LA bupivacaine, this pulse protocol is applicable, because recovery from block is slow (e.g., see

Fig. 4). The conditioning prepulse duration of 10 s was required to reach steady-state binding of cocaine to inactivated channels. Under these conditions, however, a significant number of slow inactivated channels were induced in some mutations at more positive potentials.

Local anesthetic block in our study was conventionally determined by measuring the peak amplitudes of Na^+ currents in the presence of LAs with respect to control. However, significant open-channel block occurring in the time preceding the peak may confound the estimation of block of resting and inactivated channels. For wild-type Na^+ channels, open-channel block in this time frame was negligible (data not shown). Open channel block was not analyzed in detail for the mutant channels.

Results

State-Dependent Block of μ1 Wild-Type Na^+ Channels toward Bupivacaine Enantiomers. We applied the three-step protocol (see Fig. 1B, inset, and *Materials and Methods*) in the absence and presence of 100 μM R(+)- or S(−)-bupivacaine to initially assess steady-state block of μ1 wild-type Na^+ channels. Conditioning prepulse potentials ranged in amplitude from −160 to −50 mV. Figure 1A shows μ1 wild-type Na^+ currents in the absence of drugs and in the presence of 100 μM R(+)- and S(−)-bupivacaine after conditioning prepulses to −140 or −70 mV. Both enantiomers blocked the current to a similar degree after the prepulse to −140 mV. The block was greater after the prepulse to −70 mV and more so for R(+)-bupivacaine than for S(−)-bupivacaine.

Figure 1B shows normalized μ1 wild-type currents as a function of the conditioning prepulse potential. Slow inactivation was detectable in control records after prepulses more positive than −100 mV. Block by 100 μM R(+)- and S(−)-bupivacaine reached plateaus at potentials ≤−140 and ≥−70 mV, confirming the existence of two distinguishable binding affinities for both bupivacaine enantiomers that are revealed by the pulse protocol (Wright et al., 1997).

To determine more accurately the potencies of bupivacaine enantiomers in blocking resting and inactivated channels, IC_{50} values were determined in concentration-inhibition experiments for both enantiomers; we chose conditioning prepulses to −140 and −70 mV, corresponding to block of resting and inactivated channels, respectively (Fig. 1C). The IC_{50} values for block by R(+)- and S(−)-bupivacaine were 160 ± 21 and 146 ± 14 μM, respectively, for resting channels and 8.6 ± 0.5 and 12 ± 1 μM, respectively, for inactivated channels. The Hill coefficients were close to unity, which suggests a single binding site for bupivacaine enantiomers in μ1 wild-type Na^+ channels. The stereopotency ratios for R(+)- over S(−)-bupivacaine were significantly different between resting (0.9) and inactivated channels (1.4; $p < .05$). These results confirm previous reports that Na^+ channels display only weak stereoselectivity toward bupivacaine enantiomers (Wang and Wang, 1992; Valenzuela et al., 1995).

The residue μ1-N434 in D1-S6 of μ1 wild-type Na^+ channels is asparagine (N). Asparagine has an uncharged side chain but is decidedly polar and thus is a hydrophilic amino acid. By using site-directed mutagenesis, we made a series of amino acid substitutions at position μ1-N434 that vary the hydrophobicity, aromaticity, polarity, and charge at this site. We chose alanine (A) as a small aliphatic, hydrophobic residue; the aromatic residues phenylalanine (F), tryptophan (W), and tyrosine (Y); the hydroxyl- or sulfur-containing, and therefore polar, residues threonine (T) and cysteine (C); the acidic, negatively charged residue aspartic acid (D); and the positively charged residues lysine (K) and arginine (R). All mutants expressed sufficient Na^+ currents in HEK 293t cells for pharmacological analysis.

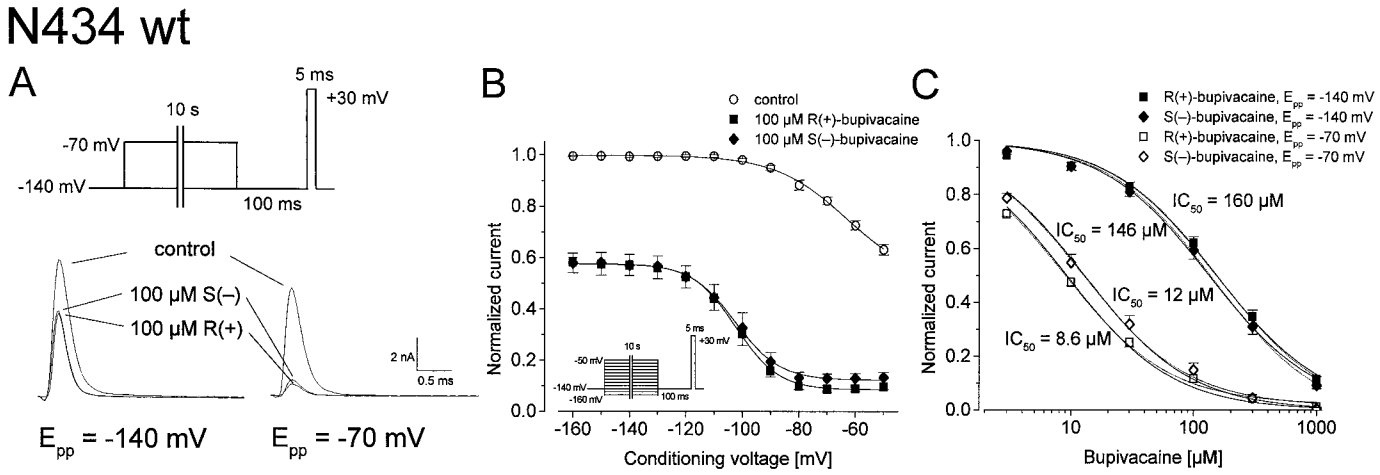

Fig. 1. State-dependent block of μ1 Na^+ channels by bupivacaine enantiomers. A, μ1 wild-type Na^+ currents in control and in the presence of 100 μM R(+)- or S(−)-bupivacaine. A 10-s conditioning prepulse (E_{pp}) to −140 or −70 mV was applied. Then a 100-ms interval at the holding potential of −140 mV was inserted before delivery of the test pulse to +30 mV to evoke the Na^+ currents. B, normalized μ1 wild-type Na^+ currents as a function of conditioning prepulse potential. Conditioning prepulses (10 s) ranging in amplitude from −160 to −50 mV were applied; then 100-ms intervals at the holding potential of −140 mV were inserted before delivery of the test pulses to +30 mV to evoke the Na^+ currents. Pulses were delivered at 30-s intervals. Control currents (○) were normalized to the current obtained with a prepulse to −160 mV. The control data for experiments with R(+)- (■) and S(−)-bupivacaine (♦) were combined. Currents obtained in the presence of 100 μM R(+)- or S(−)-bupivacaine were normalized to the current obtained in control with the corresponding prepulse potential. Solid lines represent fits of the data to a Boltzmann function. The average midpoint ($S'_{0.5}$) and slope values ($k_{S'}$) are given in Table 1. C, concentration dependence of block of resting and inactivated μ1 wild-type Na^+ channels by R(+)-bupivacaine (squares) and S(−)-bupivacaine (diamonds). The same pulse protocol as described in A was used with conditioning prepulses to −140 mV for block of resting channels (solid symbols) and −70 mV for block of inactivated channels (open symbols). Pulses were delivered at 30-s intervals. The peak amplitudes of Na^+ currents were measured in different drug concentrations, normalized with respect to the peak amplitude in control and plotted against the drug concentration. Dotted lines represent fits to the data with the Hill equation. Solid lines are fits with the Hill coefficient set to 1. Half-maximum inhibiting concentrations (IC_{50}) as well as Hill coefficients are given in Table 2.

We did not aim for a detailed analysis of the gating properties of the channels in the present study. Activation kinetics were not measured because activation, in contrast to steady-state inactivation, was shown to play a minor role in modulation of LA affinity (Wright et al., 1999). However, we briefly characterized fast and slow inactivation of μ1-N434 mutant channels.

Fast and Slow Inactivation of μ1-N434 Mutant Channels. A conventional two-pulse protocol was used to determine the voltage dependence of fast inactivation (Fig. 2A, inset). The $V_{0.5}$ values for μ1-N434T and μ1-N434R channels showed no statistically significant difference compared with μ1 wild-type channels. The $V_{0.5}$ values for μ1-N434Y, μ1-N434C, μ1-N434W, μ1-N434F, and μ1-N434D were shifted to more negative potentials by 32.1, 16.7, 16.1, 14.2, and 5.2 mV, respectively. The $V_{0.5}$ values for μ1-N434K and μ1-N434A were shifted to more positive potentials by 4.4 and 12.6 mV, respectively (Table 1).

Figure 2B shows the effect of the pulse protocol used to assess steady-state block at various 10-s prepulse potentials on μ1 wild-type and mutant Na^+ channels in control solution. Prepulses more positive than −100 mV began to induce slow inactivation in μ1 wild-type channels. μ1-N434D and μ1-N434K exhibited similar and μ1-N434R less slow inactivation. In μ1-N434Y currents, slow inactivation was detectable at prepulses more positive than −140 mV and in μ1-N434C, μ1-N434F, and μ1-N434W currents at prepulses more positive than −120 mV. Slow inactivation increased gradually with more positive potentials. In μ1-N434A and μ1-N434T, currents slow inactivation was detectable at prepulses more positive than −90 mV and increased steeply with more positive potentials. All of these data were fitted by a Boltzmann equation. The midpoint potentials $S'_{0.5}$ and the corresponding slope factors $k_{S'}$ for control data and data obtained in the presence of 10 or 100 μM R(+)- and S(−)-bupivacaine (not shown) are given in Table 1.

It is noteworthy that the $S'_{0.5}$ values may not represent the true steady-state slow inactivation because the conditioning prepulse duration of 10 s may be too short to allow all mutants to equilibrate to their slow inactivation state. The $S'_{0.5}$ values characterize the slow inactivation specifically induced by the pulse protocol applied in this study to measure steady-state block. The results confirm previous reports that a mutation at μ1-N434 position can strongly influence both fast and slow inactivation properties of μ1 Na^+ channels (Wang and Wang, 1997).

State-Dependent Block of μ1 Na^+ Channels by Bupivacaine Enantiomers. For all mutant channels, steady-state block by bupivacaine enantiomers was first assessed at different prepulse potentials, as described above. Blocking potencies for resting and inactivated channels were subsequently determined in concentration-inhibition experiments with prepulses at which block reached a plateau (that is, a point at which inhibition did not further decrease with more negative prepulses, for resting channels, or increase with more positive prepulses, for inactivated channels). For wild-type and all mutant channels, a prepulse potential of −140 mV was deemed sufficient to estimate the bupivacaine potencies for resting channels, with the exception of μ1-N434Y and μ1-N434C, for which −160 mV was used. Potencies for inactivated channels were all estimated with a prepulse potential of −70 mV, at which block of μ1 wild-type, μ1-N434T, μ1-N434D, μ1-N434K, and μ1-N434R clearly approached a plateau. However, at prepulse potentials more positive than −70 mV, block of μ1-N434A channels decreased slightly. Maximum block of μ1-N434Y, μ1-N434W, μ1-N434C, and μ1-N434F channels was already induced at potentials of −90 and −80 mV, respectively, and decreased slightly with more positive potentials, so we may have underestimated block of inactivated channels in these mutations.

The decrease in block at the very positive potentials in some mutants may be a result of channel activation and knockout of the drug by accumulated external Na^+ ions

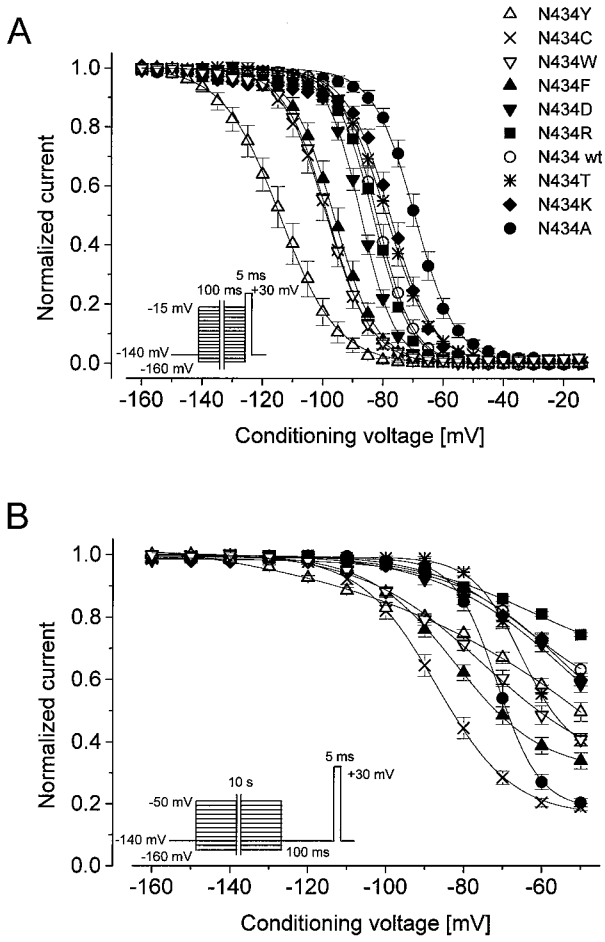

Fig. 2. Inactivation kinetics of μ1 wild-type and mutant Na^+ channels. A, voltage dependence of fast inactivation. Wild-type and mutant Na^+ currents were evoked by a 5-ms test pulse to +30 mV after 100-ms conditioning prepulses (V_{pp}) between −160 and −15 mV in 5-mV increments (see inset). Pulses were delivered at 20-s intervals. Holding potential was −140 mV. The currents were normalized with respect to the current obtained after a prepulse to −160 mV, plotted against the prepulse potential, and fitted to a Boltzmann equation $\{1/1 + \text{epx}[(V_{pp} - V_{0.5})/k]\}$. $V_{0.5}$ is the voltage at which 50% of channels are unavailable, and k is the slope factor. All values are given in Table 1. B, normalized μ1 wild-type and mutant Na^+ currents in control as a function of conditioning prepulse potential as used to assess steady-state block. Conditioning prepulses (E_{pp}; 10-s) ranging in amplitude from −160 to −50 mV were applied; then, 100-ms intervals at the holding potential of −140 mV were inserted before delivery of the test pulses to +30 mV to evoke the Na^+ currents (see inset). Pulses were delivered at 30-s intervals. Currents were normalized to the current obtained with a prepulse to −160 mV, plotted against the prepulse potential, and fitted to a Boltzmann equation $\{((A_1 - A_2)/(1 + \text{epx}((E_{pp} - S'_{0.5})/k_{S'})) + A_2\}$. $S'_{0.5}$ is the midpoint potential for inactivation under this impulse protocol, and $k_{S'}$ is the slope factor. All control values as well as the values obtained in the presence of 10 or 100 μM R(+)- and S(−)-bupivacaine are given in Table 1.

(Wang, 1988) and/or of the contribution of slow inactivated channels to bupivacaine block. It was beyond the scope of the present study to determine quantitatively the relative contribution of open and slow inactivated states to the binding affinity at the critical potentials. When comparing IC_{50} values of mutations μ1-N434Y, μ1-N434W, μ1-N434C, and μ1-N434F obtained at a prepulse potential of −70 mV with other mutants, however, one should keep this limitation in mind.

The effects of 100 μM R(+)- and S(−)-bupivacaine on wild-type and mutant Na^+ currents elicited after prepulses to −140 and −70 mV are shown in Fig. 3A and the IC_{50} values resulting from concentration-inhibition experiments are summarized in Fig. 3, B and C. The channels are arranged from top to bottom traces (Fig. 3A) and from left to right (Fig. 3, B and C) according to their hydropathy index beginning with the most hydrophobic substitutions. All IC_{50} values and Hill coefficients are also listed in Table 2, along with calculated ratios for state-selective and stereoselective potencies.

In resting channels, the blocking potency of R(+)- and S(−)-bupivacaine was increased in all mutant channels. This increase was the smallest (<1.5-fold) for mutations μ1-N434K and μ1-N434R, containing positively charged residues, and moderate (about 2-fold) for mutation μ1-N434D and μ1-N434A, containing a negatively charged or a small hydrophobic residue, respectively. Mutations containing a polar residue (μ1-N434T and μ1-N434C) showed a 2.5- to 6-fold increase in blocking potency, and mutations containing an aromatic residue (μ1-N434F, μ1-N434W, and μ1-N434Y) seemed to have the highest sensitivity to block of both resting and inactivated states by bupivacaine enantiomers.

In inactivated channels, the increase in potency was greater for mutation μ1-N434D than for mutations μ1-N434C and μ1-N434T. Potency was decreased in mutation μ1-N434K. The potency to block inactivated μ1-N434R channels decreased for S(−)-bupivacaine but remained constant for R(+)-bupivacaine, resulting in a stereoselectivity (stereopotency ratio) of 3 for R(+)- over S(−)-bupivacaine (Table 2) for the inactivated state of μ1-N434R channels.

Recovery of Inactivated μ1-N434R Channels from Block by Bupivacaine Enantiomers. Different rates of dissociation of R(+)- and S(−)-bupivacaine from inactivated μ1-N434R Na^+ channels during the interval at −140 mV before the test pulse may confound the estimation of block of inactivated channels at −70 mV. Therefore, we determined the percentage of block of inactivated μ1 wild-type and μ1-N434R channels and their recovery time course from block by bupivacaine enantiomers (Fig. 4).

Currents in the absence of drugs and in the presence of 100 μM R(+)- or S(−)-bupivacaine recovered with fast (τ_1) and slow time constants (τ_2). In the presence of a drug, τ_1 reflects the fast recovery from inactivation of unblocked channels; τ_2 reflects the slow dissociation of drug from channels that were blocked during the conditioning prepulse, including rebinding and dissociation from resting channels and slow recovery from inactivation seen also under control conditions. Control currents of mutation μ1-N434R (Fig. 4B) recovered from a 10-s prepulse to −70 mV with fast and slow time constants of 4.6 ± 0.9 ms and 1.1 ± 0.2 s, respectively. In the presence of 100 μM R(+)-bupivacaine, these channels recovered with fast and slow time constants of 6.2 ± 0.2 ms and 2.8 ± 0.1 s, respectively, and in 100 μM S(−)-bupivacaine with respective values of 4.7 ± 1.2 ms and 1.7 ± 0.1 s. The fractional amplitudes of the slow phase of recovery for R(+)- and S(−)-bupivacaine were 92 and 73%, respectively, resulting from the different potencies of bupivacaine enantiomers to block inactivated μ1-N434R channels. The slow time constant for recovery from R(+)-bupivacaine block was 1.6-fold longer than that for S(−)-bupivacaine. More importantly, the results clearly show that at 100-ms recovery time, little recovery of inactivated drug-bound channels had occurred, thus confirming the significant difference in block by R(+)- and

TABLE 1

Parameters for inactivation kinetics of μ1 wild-type and mutant Na^+ channels

The values for the voltage dependence of fast inactivation $V_{0.5}$ and k (mean ± S.E., n = number of experiments) and the slow inactivation $S'_{0.5}$ and $k_{s'}$ (fitted values ± S.E.) in the absence and presence of 100 μM (μl wild-type, μl-N434A, μl-N434T, μl-N434D, μl-N434K, μl-N434R) or 10 μM (μl-N434C, μl-N434F, μl-N434Y, μl-N434W) bupivacaine enantiomers were determined as described in Fig. 2.

Channel	Control		Control		R(+)-Bupivacaine		S(−)-Bupivacaine	
	$V_{0.5}$	k	$S'_{0.5}$	$k_{S'}$	$S'_{0.5}$	$k_{S'}$	$S'_{0.5}$	$k_{S'}$
				mV				
Wild-type	−82.1 ± 1.4	5.4 ± 0.1 (n = 10)	−63.0 ± 2.5	12.7 ± 1.1 (n = 22)	−102.3 ± 0.5	7.6 ± 0.4 (n = 11)	−102.5 ± 0.6	7.9 ± 0.5 (n = 11)
N434A	−69.5 ± 1.4	6.8 ± 0.4 (n = 4)	−71.4 ± 0.1	5.5 ± 0.9 (n = 21)	−97.9 ± 1.9	5.3 ± 1.7 (n = 10)	−94.9 ± 1.6	4.9 ± 1.3 (n = 11)
N434F	−96.3 ± 1.8	6.3 ± 0.2 (n = 11)	−82.2 ± 0.7	11.7 ± 0.6 (n = 17)	−111.5 ± 2.7	6.8 ± 2.4 (n = 4)	−113.8 ± 4.3	7.1 ± 3.7 (n = 4)
N434W	−98.2 ± 0.4	7.4 ± 0.3 (n = 5)	−74.4 ± 2.0	16.0 ± 1.2 (n = 9)	−115.7 ± 1.6	9.2 ± 1.5 (n = 5)	−115.5 ± 2.6	7.1 ± 2.3 (n = 4)
N434Y	−114.2 ± 2.7	8.6 ± 0.1 (n = 7)	−36.6 ± 30.6	36.8 ± 8.7 (n = 8)	−133.5 ± 3.4	9.1 ± 2.7 (n = 4)	−139.0 ± 5.3	9.3 ± 3.7 (n = 4)
N434T	−78.9 ± 1.2	7.3 ± 0.2 (n = 7)	−65.2 ± 0.3	6.2 ± 0.2 (n = 11)	−105.5 ± 2.3	8.5 ± 2.1 (n = 5)	−99.5 ± 1.9	7.8°1.7 (n = 6)
N434C	−98.8 ± 1.9	6.4 ± 0.2 (n = 10)	−86.9 ± 0.3	9.7 ± 0.3 (n = 25)	−124.0 ± 7.5	6.8 ± 6.5 (n = 11)	−119.5 ± 5.7	4.2 ± 5.8 (n = 10)
N434D	−87.3 ± 0.8	5.6 ± 0.4 (n = 5)	−53.3 ± 9.1	16.8 ± 2.7 (n = 20)	−110.9 ± 0.8	9.2 ± 0.7 (n = 11)	−111.6 ± 0.6	8.4 ± 0.5 (n = 9)
N434K	−77.7 ± 1.3	7.0 ± 0.4 (n = 9)	−54.0 ± 6.6	14.4 ± 2.0 (n = 15)	−88.9 ± 1.1	5.9 ± 1.0 (n = 8)	−92.6 ± 1.6	7.3 ± 1.4 (n = 7)
N434R	−83.3 ± 0.5	6.1 ± 0.1 (n = 9)	−62.6 ± 5.9	15.8 ± 2.5 (n = 16)	−97.1 ± 0.6	9.6 ± 0.5 (n = 8)	−92.2 ± 0.7	9.8 ± 0.6 (n = 8)

S(−)-bupivacaine and validating the pulse protocol used to estimate block of inactivated μ1-N434R channels.

Because of the large fraction of inactivated channels blocked by either 100 μM R(+)- or S(−)-bupivacaine (>90%), no reliable fast time constants could be estimated for μ1 wild-type channels (Fig. 4A). Dissociation from blocked μ1 wild-type channels was slower for both R(+)- and S(−)-bupivacaine (4.4 ± 0.1 and 2.3 ± 0.1 s, respectively) than the corresponding dissociation from μ1-N434R channels. It is noteworthy that the recovery from block by R(+)-bupivacaine was about two times slower than from block by S(−)-bupivacaine, although stereoselectivity was weak for both resting and inactivated μ1 wild-type channels, revealing that stereoselective actions are not determined by differences in dissociation kinetics alone.

Block of μ1-N434R Na^+ Channels by Other LA Stereoisomers. We were interested in whether the increased stereoselectivity for bupivacaine of inactivated μ1-N434R channels also occured with other LA stereoisomers. Therefore, we assessed steady-state block of μ1 wild-type and μ1-N434R channels by (+)- and (−)-cocaine and by the enantiomers of the LA compound RAC 109. All IC_{50} values and Hill coefficients for block by cocaine-enantiomers are listed in Table 3.

As shown in Fig. 5, A and B, block of inactivated μ1 wild-type channels by cocaine enantiomers displayed higher stereoselectivity than block by bupivacaine enantiomers (2.4 versus 1.4, respectively). Block of resting μ1-N434R channels by cocaine enantiomers was decreased slightly compared with that of resting μ1 wild-type channels, in contrast to block of resting channels by bupivacaine enantiomers, which was slightly increased. However, the potency to block inactivated channels was selectively decreased for (+)-cocaine in mutation μ1-N434R, resulting in a stereoselectivity (stereopotency ratio) of 4 for (−)-cocaine over (+)-cocaine (Table 3). Hence, the differential reduction in blocking potency of inactivated μ1-N434R channels toward one stereoisomer is consistent for both bupivacaine and cocaine.

The effects of RAC 109 enantiomers on μ1 wild-type and μ1-N434R Na^+ channels are shown in Fig. 5C. Both resting and inactivated wild-type μ1 Na^+ channels showed a moderate and similar stereoselectivity toward the RAC 109 enantiomers. In μ1-N434R channels, the potency for RAC 109 enantiomers was reduced for both resting and inactivated channels and stereoselectivity became minimal for both states. This result demonstrates that μ1-N434R is involved differently in RAC 109 stereoselectivity compared with bupivacaine and cocaine.

Discussion

Our data demonstrate that most point mutations at μ1-N434 had significant effects on both fast and slow inactiva-

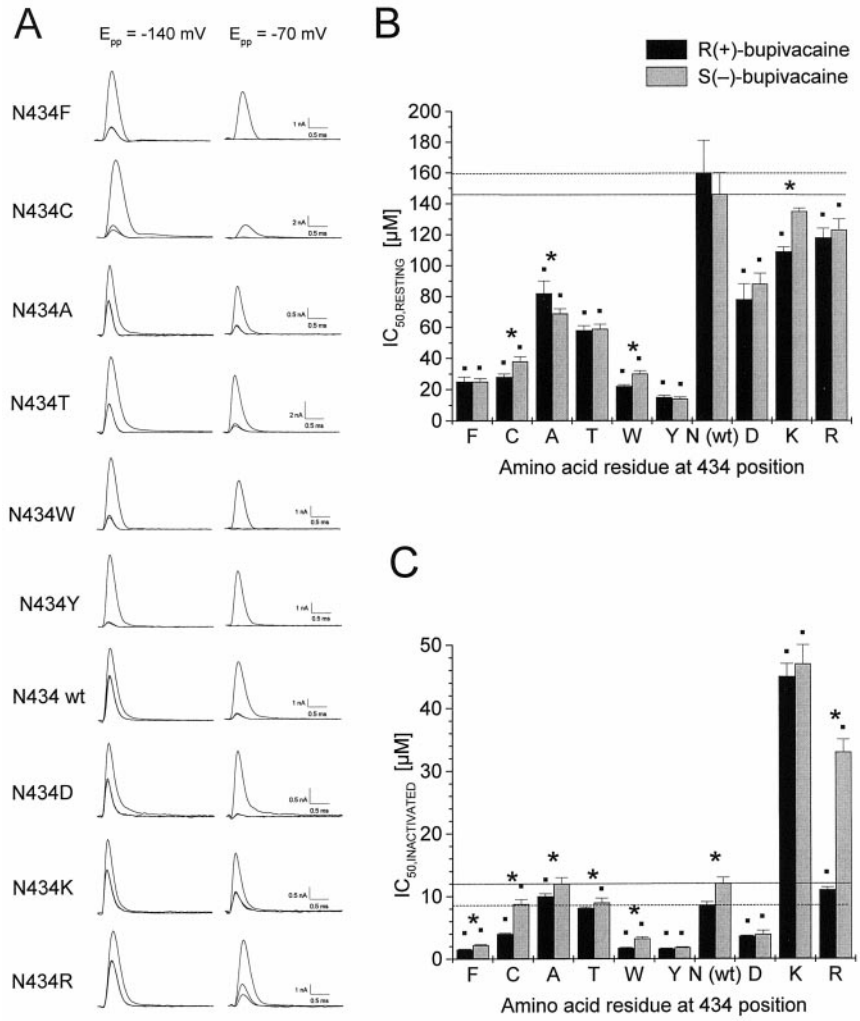

Fig. 3. State-dependent block of μ1 mutant and wild-type Na^+ channels by bupivacaine enantiomers. A, mutant and wild-type Na^+ currents in control (larger currents in each set of traces) and in the presence of 100 μM R(+)- and S(−)-bupivacaine (smaller currents in each set of traces). The same pulse protocol as described in Fig. 1A was used with conditioning prepulses to −140 mV for block of resting channels (E_{pp} = −140 mV, left column) and −70 mV for block of inactivated channels (E_{pp} = −70 mV, right column). Note the clearly separable currents in the presence of 100 μM R(+)- and S(−)-bupivacaine elicited with E_{pp} = −70 mV in mutation N434R. B and C, affinities of resting (B) and inactivated (C) μ1 wild-type and mutant μ1 Na^+ channels toward bupivacaine enantiomers. The IC_{50} values (fitted values ± S.E.M.) were obtained as described in Fig. 1C with the exception of the IC_{50} value for the resting state of μ1-N434Y and μ1-N434C, which were determined with conditioning prepulses to −160 mV. The channels are plotted from left to right according to their hydropathy index (Kyte and Doolittle, 1982): F, 2.8; C, 2.5; A, 1.8; T, −0.7; W, −0.9; Y, −1.3; N, −3.5; D, −3.5; K, −3.9; R, −4.5. ∗ between two columns indicates a statistically significant difference in IC_{50} values between R(+)- and S(−)-bupivacaine ($p < .05$). ■ above a column indicates a statistically significant change in IC_{50} values for the enantiomer compared with the corresponding IC_{50} value in the wild-type ($p < .05$). The dashed and dotted lines were drawn according to the IC_{50} values of wild-type for R(+)- and S(−)-bupivacaine, respectively.

tion of Na^+ currents and on potencies of bupivacaine enantiomers to block resting and inactivated channels. In the following, we equate the term binding affinity with blocking potency measured in concentration-inhibition experiments when appropriate. We thereby assume that block of Na^+ channels by LAs measured in electrophysiological experiments directly reflects binding of LAs to their site.

Changes in Fast and Slow Inactivation. Mutations μ1-N434Y, μ1-N434F, μ1-N434W, μ1-N434C, and μ1-N434A had the most dramatic effects on both fast and slow inactivation. All of them enhanced slow inactivation, as shown in the leftward shift of the S'_∞ curve. However, μ1-N434Y, μ1-N434W, μ1-N434F, and μ1-N434C shifted the voltage dependence of fast inactivation (h_∞) to the hyperpolarizing direction, whereas μ1-N434A shifted it to the depolarizing direction. These data together demonstrate that fast and slow inactivation can be differentially modulated through substitution of residue N434.

Several molecular structures are known to be involved in fast inactivation of Na^+ channels, including the intracellular loop between D3 and D4 (Stühmer et al., 1989; West et al., 1992) and amino acid residues near the intracellular end of D4-S6 (McPhee et al., 1994) and within the short intracellular loop between D4-S4 and D4-S5 (McPhee et al., 1998). However, numerous mutations in other regions of the Na^+ channel protein are known to modulate fast inactivation as well.

Less is known about the molecular structures that govern slow inactivation of Na^+ channels, although there is growing evidence for an important role of segments S6. Enhancement of slow inactivation (Fig. 2B), together with positive shifts in the voltage dependence of activation and fast inactivation in mutation μ1-N434A in D1-S6, has been described (Wang and Wang, 1997). A mutation of an external pore-flanking residue in D1-S6 eliminated the anomalous slow recovery from inactivation of the α subunit of μ1 Na^+ channels expressed in *X. laevis* oocytes (Balser et al., 1996a). Both reports point out the functional and structural analogy of slow inactivation in Na^+ channels to the C-type inactivation in homotetrameric *Shaker* K^+ channels that is modulated by external pore-lining residues and by residues in segment S6 (Hoshi et al., 1991; Boland et al., 1994; Yellen et al., 1994). Interestingly, segment S6 in *Shaker* K^+ channels may be involved in the activation-gating mechanism as well (Liu et al., 1997; Holmgren et al., 1998). Whether segment D1-S6 of the Na^+ channel plays a comparable role in channel gating remains unanswered.

Changes in Bupivacaine Affinity. As in the wild-type, two distinguishable bupivacaine binding affinities corresponding to the resting and inactivated states were found in all mutant channels. Mutations of N434 clearly affected binding of LAs to resting and inactivated channels differently.

In theory, three possible mechanisms may explain altered LA affinities: 1) mutations at N434 alter the gating properties and consequently affect state-dependent binding; (2) mutations at N434 influence LA binding by indirect allosteric effects at the site; or 3) residues at N434 directly interact with LA in binding to the Na^+ channel.

TABLE 2

IC_{50} values for bupivacaine block of resting and inactivated μl wild-type and mutant Na^+ channels

The IC_{50} values (fitted values ± S.E.) for the resting ($IC_{50,R}$) and inactivated states ($IC_{50,I}$) were obtained as described in Fig. 1C with the exception of the $IC_{50,R}$ value for μl-N434C and μl-N434Y, which were determined with conditioning prepulses to −160 mV. Hill coefficients are listed in brackets.

Channel	$IC_{50,R}$			$IC_{50,I}$			$IC_{50,R}/IC_{50,I}$	
	R(+)-Bupivacaine	S(−)-Bupivacaine	Ratio S(−)/R(+)	R(+)-Bupivacaine	S(−)-Bupivacaine	Ratio S(−)/R(+)	R(+)-Bupivacaine	S(−)-Bupivacaine
	μM			*μM*				
Wild-type	160 ± 21 (n = 7) [1.02 ± 0.04]	146 ± 14 (n = 5) [1.03 ± 0.03]	0.9	8.6 ± 0.5 (n = 6) [0.98 ± 0.01]	12 ± 1 (n = 5) [0.99 ± 0.02]	1.4	18.6	12.2
N434A	82 ± 8 (n = 7) [0.97 ± 0.06]	69 ± 3 (n = 8) [1.12 ± 0.05]	0.8	10 ± 0.4 (n = 7) [0.81 ± 0.03]	12 ± 1 (n = 6) [0.89 ± 0.05]	1.2	8.2	5.8
N434F	25 ± 3 (n = 5) [0.97 ± 0.09]	25 ± 2 (n = 3) [1.04 ± 0.08]	1.0	1.5 ± 0.1 (n = 4) [0.99 ± 0.06]	2.2 ± 0.1 (n = 4) [1.18 ± 0.06]	1.5	16.7	11.4
N434W	22 ± 1 (n = 4) [1.12 ± 0.06]	30 ± 2 (n = 4) [1.06 ± 0.07]	1.4	1.7 ± 0.1 (n = 4) [1.19 ± 0.08]	3.2 ± 0.3 (n = 4) [1.09 ± 0.12]	1.9	12.9	9.4
N434Y	15 ± 1 (n = 4) [0.98 ± 0.06]	14 ± 1 (n = 4) [1.02 ± 0.06]	0.9	1.6 ± 0.1 (n = 4) [1.15 ± 0.02]	1.8 ± 0.1 (n = 4) [1.14 ± 0.11]	1.1	9.4	7.8
N434T	58 ± 3 (n = 4) [1.12 ± 0.06]	59 ± 3 (n = 5) [1.14 ± 0.07]	1.0	8.1 ± 0.2 (n = 5) [0.85 ± 0.02]	9.0 ± 0.7 (n = 4) [0.94 ± 0.07]	1.1	7.2	6.6
N434C	28 ± 2 (n = 5) [1.08 ± 0.09]	38 ± 3 (n = 9) [1.15 ± 0.10]	1.4	4.0 ± 0.1 (n = 5) [1.00 ± 0.02]	8.8 ± 0.7 (n = 13) [0.87 ± 0.06]	2.2	7.0	4.3
N434D	78 ± 10 (n = 5) [0.92 ± 0.10]	88 ± 7 (n = 7) [1.15 ± 0.10]	1.1	3.6 ± 0.1 (n = 4) [1.06 ± 0.02]	3.9 ± 0.6 (n = 5) [1.01 ± 0.16]	1.1	21.7	22.6
N434K	109 ± 3 (n = 7) [0.99 ± 0.03]	135 ± 2 (n = 6) [1.05 ± 0.01]	1.2	45 ± 2 (n = 5) [0.99 ± 0.04]	47 ± 3 (n = 6) [0.92 ± 0.05]	1.0	2.4	2.9
N434R	118 ± 6 (n = 7) [1.01 ± 0.04]	123 ± 7 (n = 8) [1.00 ± 0.05]	1.0	11 ± 0.4 (n = 7) [0.95 ± 0.03]	33 ± 2 (n = 6) [0.93 ± 0.05]	3.0	10.7	3.7

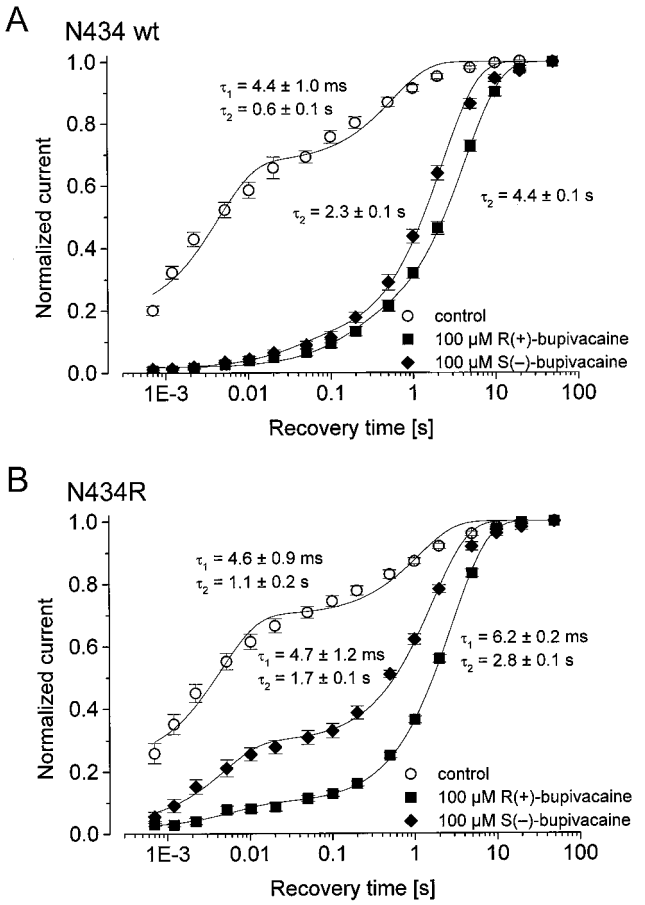

Fig. 4. Recovery from block of inactivated μ1 wild-type and μ1-N434R Na^+ channels by bupivacaine enantiomers. Cells were conditioned with a 10-s depolarizing pulse to −70 mV from a holding potential of −140 mV. Recovery was determined by applying a test pulse to +30 mV at various times after the conditioning pulse. The data were normalized to the amplitude of the test pulse obtained after 50-s recovery time. The data were best fitted by the sum of two exponentials. The control data (○) for experiments with R(+)- and S(−)-bupivacaine were combined. A, μ1 wild-type currents in the absence of drugs (○) recoverd with fast (τ_1) and slow time constants (τ_2) of 4.4 ± 1.0 ms and 0.6 ± 0.1 s, respectively. Because of the large fraction of inactivated channels blocked by either 100 μM R(+)- or S(−)-bupivacaine (>90%), no reliable τ_1 could be estimated for μ1 wild-type channels. Inactivated μ1 wild-type channels recovered from block by R(+)-bupivacaine (■; n = 5) with τ_2 = 4.4 ± 0.1 s and from block by S(−)-bupivacaine (◆; n = 5) with τ_2 = 2.3 ± 0.1 s. B, μ1-N434R currents in the absence of drugs (○) recoverd with τ_1 = 4.6 ± 0.9 ms and τ_2 = 1.1 ± 0.2 s. Inactivated μ1-N434R channels recovered from block by R(+)-bupivacaine (■; n = 8) with τ_1 = 6.2 ± 0.2 ms and τ_2 =2.8 ± 0.1 s and from block by S(−)-bupivacaine (◆; n = 7) with τ_1 = 4.7 ± 1.2 ms and τ_s = 1.7 ± 0.1 s. The fractional amplitudes of the slow phase of recovery for R(+)- and S(−)-bupivacaine were 92 and 73%, respectively.

Mutations at N434 indeed had marked effects on gating properties of the channels. However, shifts in the voltage dependence of steady-state inactivation elicited linear shifts in the voltage dependence of steady-state block but did not affect LA affinity of resting and inactivated channels (Wright et al., 1999). In the present study, affinities of resting and inactivated channels toward LAs were determined outside the potential range (−120 to −80 mV) where resting-to-inactivated transitions occur in the presence of bupivacaine enantiomers and should not be influenced by shifts in the voltage dependence of fast inactivation.

Affinities of inactivated channels were estimated with conditioning prepulses to −70 mV, a potential that induced considerably different percentages of slow inactivated channels in the mutants. Consequently, slow-inactivated channels may contribute to LA block. Slow-inactivated states of μ1 Na^+ channel α subunits expressed in *X. laevis* oocytes were shown to have lidocaine affinity comparable with that of fast-inactivated states in $\alpha\beta_1$ coexpressed channels (Balser et al., 1996b). It is unclear, however, whether the slow-inactivated states observed in oocytes and in mammalian expression systems are comparable.

Ultimately, based on our results, we could not discern a clear relationship between shifts in fast or slow inactivation in mutant channels and their resting and inactivated affinities toward bupivacaine (Tables 1 and 2). Altogether, it seems that the altered LA binding affinities are not caused by the altered gating properties in mutant channels.

At present, we cannot exclude allosteric effects at the LA site caused by mutations in N434 as an explanation for changes in affinity. However, there is compelling structure-function evidence for a direct interaction of N434 with bupivacaine enantiomers, as is most apparent in changes in the affinity of inactivated mutant channels. Bupivacaine affinity of inactivated channels was enhanced for mutations in the order μ1-N434Y, μ1-N434F, μ1-N434W, μ1-N434D, and μ1-N434C, whereas it was decreased for mutations μ1-N434K and μ1-N434R. The most likely explanation is that these residues interact directly with the positively charged amino group of bupivacaine. The aromatic residues phenylalanine, tryptophan, and tyrosine could increase affinity through cation-π electron interaction (Heginbotham and MacKinnon, 1992), as suggested for the rat brain IIA native residue F1579 and the positively charged moiety of an LA (Ragsdale et al., 1994). The negatively charged aspartic acid and the polar cysteine may interact electrostatically with the positively charged LA moiety to increase affinity. The positively

TABLE 3

IC_{50} values for cocaine block of resting and inactivated μl wild-type and μl-N434R Na^+ channels

The IC_{50} values (fitted values ± S.E.M.) for the resting ($IC_{50,R}$) and inactivated states ($IC_{50,I}$) were obtained as described in Fig. 1C. Hill coefficients are listed in brackets.

Channel	$IC_{50,R}$			$IC_{50,I}$			$IC_{50,R}/IC_{50,I}$	
	(+)-Cocaine	(−)-Cocaine	Ratio (+)/(−)	(+)-Cocaine	(−)-Cocaine	Ratio (+)/(−)	(+)-Cocaine	(−)-Cocaine
	μM			*μM*				
Wild-type	229 ± 2 (n = 7) [0.98 ± 0.01]	181 ± 5 (n = 6) [0.96 ± 0.03]	1.3	40 ± 1 (n = 6) [1.07 ± 0.03]	17 ± 0.5 (n = 6) [1.06 ± 0.03]	2.4	5.7	10.6
N434R	342 ± 13 (n = 4) [0.95 ± 0.03]	251 ± 4 (n = 4) [1.00 ± 0.02]	1.4	89 ± 5 (n = 4) [1.03 ± 0.05]	22 ± 0.6 (n = 4) [1.07 ± 0.03]	4	3.8	11.4

charged lysine and arginine decrease binding of the positively charged LA moiety by an electrostatic charge-charge repulsion. This mechanism also explains the reduced inactivated channel block by LAs in lysine point mutations at the putative LA binding site in D4-S6 (Wright et al., 1998). Consistent with a direct interaction of residues at N434 with a positively charged LA moiety is the unchanged bupivacaine affinity of inactivated channels in mutation μ1-N434A, where asparagine is replaced by the small hydrophobic alanine, and the small increase in the affinity in mutation μ1-N434T, where asparagine is replaced by the slightly polar threonine.

Surprisingly, all resting mutant channels showed a higher bupivacaine affinity than the resting wild-type channels. The changes in blocking potencies were not well correlated with the physical properties of the substituted residues.

These results might be interpreted like those regarding the phenylalanine residue in D4-S6 known to be critical for LA action, which appears to interact with LA in two different modes depending on the channel's state: in the resting state, hydrophobic interactions are more important for LA binding, whereas in the open and inactivated states, cation-π electron or aromatic-aromatic interactions are dominant (Li et al., 1999). The speculation that the orientation of the residue's

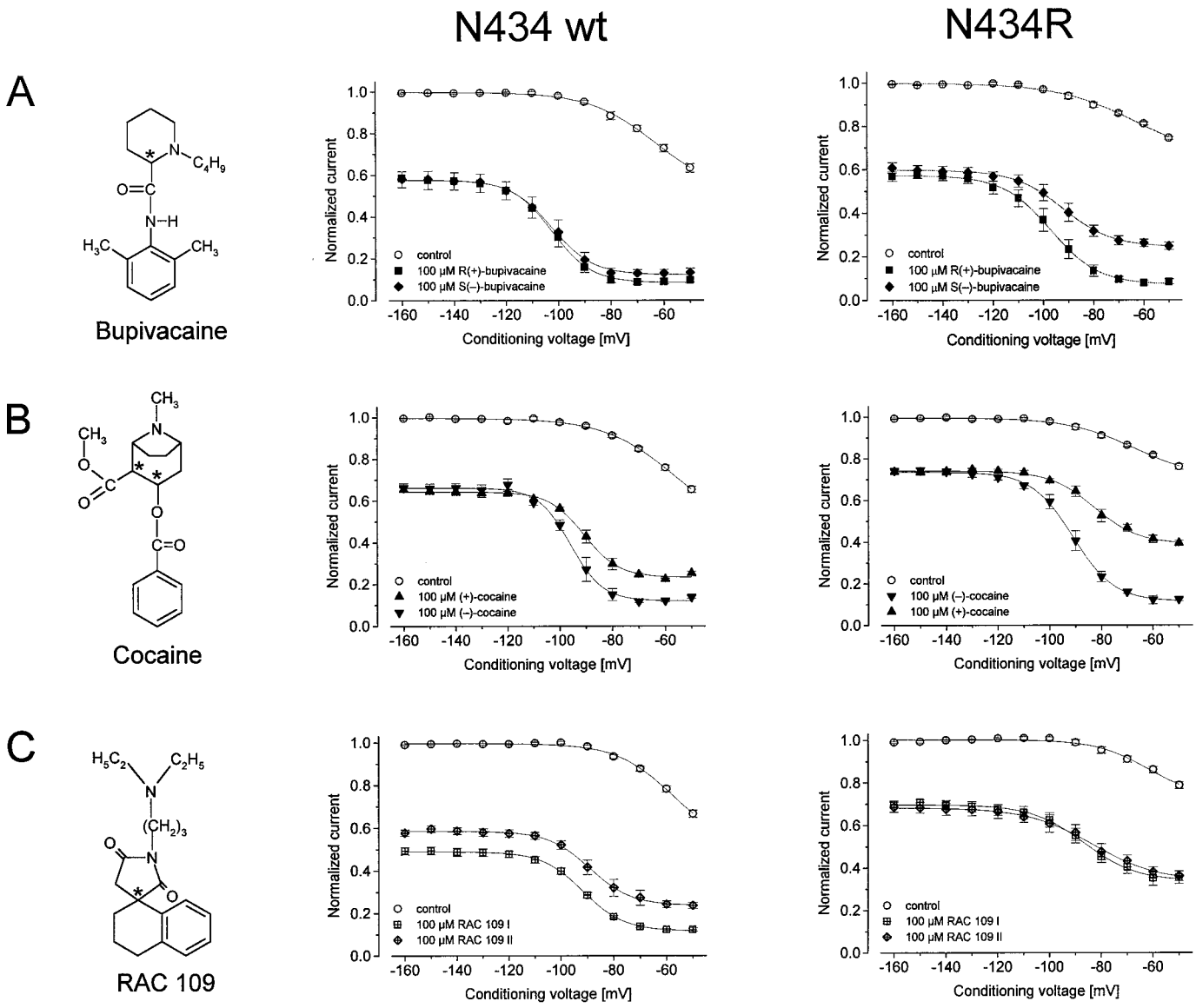

Fig. 5. State-dependent block of μ1 wild-type and μ1-N434R Na^+ currents by bupivacaine, cocaine and RAC 109 enantiomers. Normalized μ1 wild-type and μ1-N434R Na^+ currents as a function of conditioning prepulse potential in the absence (○) and presence of (A) 100 μM R(+)-bupivacaine (■) and S(−)-bupivacaine (◆), (B) 100 μM (−)-cocaine (▼) and (+)-cocaine (▲), and (C) 100 μM RAC 109 I (□) and RAC 109 II (◇). Data were obtained as described in Fig. 1B. Solid lines represent fits of a Boltzmann function to the data points as descibed in Fig. 2B. A, the average midpoint and slope values for 100 μM R(+)- and S(−)-bupivacaine in μ1 wild-type (imported from Fig. 1B for comparison) and μ1-N434R channels are given in Table 1. B, the average midpoint and slope of the Boltzman function fitted to the data for control, 100 μM (−)-cocaine, and 100 μM (+)-cocaine for μ1 wild-type channels were −56.9 ± 3.1 and 13.2 ± 1.1 mV, −96.0 ± 0.6 and 6.1 ± 0.5 mV (n = 5), and −90.9 ± 0.6 and 6.6 ± 0.6 mV (n = 5), respectively, and for μ1-N434R channels −66.6 ± 2.3 and 13.3 ± 1.2 mV, 91.0 ± 0.4 mV, and 8.0 ± 0.4 mV (n = 5) and 82.7 ± 0.8 mV and 8.7 ± 0.7 mV (n = 5), respectively. C, the average midpoint and slope of the Boltzman function for control, 100 μM RAC 109 I, and 100 μM RAC 109 II for μ1 wild-type channels were −58.1 ± 3.0 and 10.5 ± 1.2 mV, −91.7 ± 0.3 and 7.8 ± 0.3 mV (n = 8), and −89.1 ± 0.6 and 7.9 ± 0.5 mV (n = 8), respectively, and for μ1-N434R channels −61.6 ± 4.9 and 10.3 ± 2.3 mV, 86.7 ± 1.0 and 10.3 ± 0.9 mV (n = 6), and 83.2 ± 1.3 and 12.8 ± 1.1 mV (n = 7), respectively.

side chain changes in response to channel state could also apply to our results. Alternatively, mutations in N434 may nonspecifically affect LA binding to resting channels.

The role of residue N434 in LA binding to resting channels remains elusive. Nonetheless, different forces seem to regulate LA binding to resting and inactivated channels, thus suggesting that during state transitions, the LA receptor indeed alters its configuration, as implied by Hille's modulated receptor hypothesis (Hille, 1977).

What Is the Mechanism for the Altered Stereoselectivity by N434R? The most surprising result in this study was the increased stereoselectivity of inactivated μ1-N434R channels toward bupivacaine enantiomers. Resting μ1-N434R channels showed little stereoselectivity. Stereoselectivity for the inactivated state arose from a decrease in affinity for S(−)-bupivacaine with no change for R(+)-bupivacaine. Mutation μ1-N434K introduces the same positive charge, albeit of smaller dimension, yet shows no stereoselectivity.

The following inferences can be drawn from these observations. First, in the inactivated channel, residue N434 and the chiral part of the LA molecule—the amine-containing butyl piperidine ring—may be near one another, consistent with the proposed direct interaction. Second, R(+)-bupivacaine remains bound to inactivated μ1-N434R channels with minimal charge-charge repulsion, possibly because of delocalized charge in the guanidinium group of the arginine residue. Third, in addition to charge, the size and the orientation of atoms and bonds within the residue at 434 position are crucial for enhanced stereoselectivity.

The differential reduction in affinity of inactivated μ1-N434R channels toward one bupivacaine stereoisomer was also found for cocaine, which suggests that corresponding structural parts of bupivacaine and cocaine interact with the same residues. In both bupivacaine and cocaine molecules, the chiral carbon is close to the tertiary amine. In contrast, the chiral carbon of RAC 109 is located close to the aromatic part of the molecule, the moiety that might not interact with the residue at position μ1-N434. Additionally, the bulkier structure of RAC 109 may cause steric hindrance in binding to resting and inactivated μ1-N434R channels.

In conclusion, we propose that in inactivated channels, residue μ1-N434 in D1-S6 interacts directly with the positively charged moiety of the LAs bupivacaine and cocaine. Our findings provide more evidence that segments D1-S6 and D4-S6 align adjacently along the pore of the Na^+ channel, forming a domain-interface site for binding of BTX and of LAs in close proximity.

Acknowledgments

We thank to Dr. Stephen Cannon for providing the HEK 293t cell line and the CD8-pih3 m plasmid and Dr. James Trimmer for providing the μ1/skm1 plasmid.

References

Balser JR, Nuss HB, Chiamvimonvat N, Perez-Garcia MT, Marban E and Tomaselli GF (1996a) External pore residue mediates slow inactivation in μ1 rat skeletal muscle sodium channels. *J Physiol* **494:**431–442.

Balser JR, Nuss HB, Romashko DN, Marban E and Tomaselli GF (1996b) Functional consequences of lidocaine binding to slow-inactivated sodium channels. *J Gen Physiol* **107:**643–658.

Boland LM, Jurman ME and Yellen G (1994) Cysteines in the *Shaker* K^+ channel are not essential for channel activity or zinc modulation. *Biophys J* **66:**694–699.

Cannon SC and Strittmatter SM (1993) Functional expression of sodium channel mutations identified in families with periodic paralysis. *Neuron* **10:**317–326.

Catterall WA (1995) Structure and function of voltage-gated ion channels. *Annu Rev Biochem* **64:**493–531.

Cota G and Armstrong CM (1989) Sodium channel gating in clonal pituitary cells: The inactivation step is not voltage dependent. *J Gen Physiol* **94:**213–232.

Hamill OP, Marty A, Neher E, Sakmann B and Sigworth FJ (1981) Improved patch-clamp techniques for high-resolution current recording from cells and cell-free membrane patches. *Pfluegers Arch* **391:**85–100.

Heginbotham L and MacKinnon R (1992) The aromatic binding site for tetraethylammonium ion on potassium channels. *Neuron* **8:**483–491.

Hille B (1977) Local anesthetics: Hydrophilic and hydrophobic pathways for the drug-receptor reaction. *J Gen Physiol* **69:**497–515.

Hockerman GH, Peterson BZ, Johnson BD and Catterall WA (1997) Molecular determinants of drug binding and action on L-type calcium channels. *Annu Rev Pharmacol Toxicol* **37:**361–396.

Holmgren M, Shin KS and Yellen G (1998) The activation gate of a voltage-gated K^+ channel can be trapped in the open state by an intersubunit metal bridge. *Neuron* **21:**617–621.

Hondeghem LM and Katzung BG (1977) Time- and voltage-dependent interactions of antiarrhythmic drugs with cardiac sodium channels. *Biochim Biophys Acta* **472:**373–398.

Hoshi T, Zagotta WN and Aldrich RW (1991) Two types of inactivation in Shaker K^+ channels: Effects of alterations in the carboxy-terminal region. *Neuron* **7:**547–556.

Kyte J and Doolittle F (1982) A simple method for displaying the hydropathic character of a protein. *J Mol Biol* **157:**105–132.

Li H-L, Galue A, Meadows L and Ragsdale DS (1999) A molecular basis for the different local anesthetic affinities of resting versus open and inactivated states of the sodium channel. *Mol Pharmacol* **55:**134–141.

Linford NJ, Cantrell AR, Qu Y, Scheuer T and Catterall WA (1998) Interaction of batrachotoxin with the local anesthetic receptor site in transmembrane segment IVS6 of the voltage-gated sodium channel. *Proc Natl Acad Sci USA* **95:**13947–13952.

Liu Y, Holmgren M, Jurman ME and Yellen G (1997) Gated access to the pore of a voltage-dependent K^+ channel. *Neuron* **19:**175–184.

McPhee JC, Ragsdale D, Scheuer T and Catterall WA (1994) A mutation in segment IVS6 disrupts fast inactivation of sodium channels. *Proc Natl Acad Sci USA* **91:**12346–12350.

McPhee JC, Ragsdale DS, Scheuer T and Catterall WA (1998) A critical role for the S4–S5 intracellular loop in domain IV of the sodium channel alpha-subunit in fast inactivation. *J Biol Chem* **273:**1121–1129.

Ragsdale D, McPhee JC, Scheuer T and Catterall WA (1994) Molecular determinants of state-dependent block of Na^+ channels by local anesthetics. *Science (Wash DC)* **265:**1724–1728.

Stühmer W, Conti F, Suzuki H, Wang X, Noda M, Yahagi N, Kubo H and Numa S (1989) Structural parts involved in activation and inactivation of the sodium channel. *Nature (Lond)* **339:**597–603.

Sunami A, Dudley SCJ and Fozzard HA (1997) Sodium channel selectivity filter regulates antiarrhythmic drug binding. *Proc Natl Acad Sci USA* **94:**14126–14131.

Trainer VL, Brown GB and Catterall WA (1996) Site of covalent labeling by a photoreactive batrachotoxin derivative near transmembrane segment IS6 of the sodium channel α subunit. *J Biol Chem* **271:**11261–11267.

Valenzuela C, Snyders DJ, Bennett PB, Tamargo J and Hondeghem LM (1995) Stereoselective block of cardiac sodium channels by bupivacaine in guinea pig ventricular myocytes. *Circulation* **92:**3014–3024.

Wang GK (1988) Cocaine-induced closures of single batrachotoxin-activated Na^+ channels in planar lipid bilayers. *J Gen Physiol* **92:**747–765.

Wang GK, Quan C and Wang SY (1998) Local anesthetic block of batrachotoxin-resistant muscle Na^+ channels. *Mol Pharmacol* **54:**389–396.

Wang GK and Wang SY (1992) Altered stereoselectivity of cocaine and bupivacaine isomers in normal and batrachotoxin-modified Na^+ channels. *J Gen Physiol* **100:**1003–1020.

Wang SY and Wang GK (1997) A mutation in segment I-S6 alters slow inactivation of sodium channels. *Biophys J* **72:**1633–1640.

Wang SY and Wang GK (1998) Point mutations in segment I-S6 render voltage-gated Na^+ channels resistant to batrachotoxin. *Proc Natl Acad Sci USA* **95:**2653–2658.

West JW, Patton DE, Scheuer T, Wang Y, Goldin AL and Catterall WA (1992) A cluster of hydrophobic amino acid residues required for fast Na^+-channel inactivation. *Proc Natl Acad Sci USA* **89:**10910–10914.

Wright SN, Wang S-Y, Kallen RG and Wang GK (1997) Differences in steady-state inactivation between Na channel isoforms affect local anesthetic binding affinity. *Biophys J* **73:**779–788.

Wright SN, Wang S-Y and Wang GK (1998) Lysine point mutations in Na^+ channel D4–S6 reduce inactivated channel blcok by local anesthetics. *Mol Pharmacol* **54:**733–739.

Wright SN, Wang S-Y, Xiao Y-F and Wang GK (1999) State-dependent cocaine block of Na channel isoforms, chimeras, and channels coexpressed with the β1 subunit. *Biophys J* **76:**233–245.

Yellen G, Sodickson D, Chen T and Jurman ME (1994) An engineered cysteine in the external mouth of a K^+ channel allows inactivation to be modulated by metal binding. *Biophys J* **66:**1068–1075.

Zamponi GW, Doyle DD and French RJ (1993) State-dependent block underlies the tissue specificity of lidocaine action on batrachotoxin-activated cardiac sodium channels. *Biophys J* **65:**91–100.

Send reprint requests to: Dr. Carla Nau, Department of Anesthesia Research Laboratories, Brigham and Women's Hospital, 75 Francis St., Boston, MA 02115. E-mail: cnau@zeus.bwh.harvard.edu